Available online at www.sciencedirect.com
SCIENCE DIRECT®
Journal of Nuclear Materials 329–333 (2004) 502–506
journal of nuclear materials
www.elsevier.com/locate/jnucmat

# A model stress analysis of swelling in SiC/SiC composites as a function of fiber type and carbon interphase structure

Charles H. Henager Jr. [a,*], Edward A. Le [b], Russ H. Jones [a]

[a] Pacific Northwest National Laboratory, 902 Battelle Blvd., MS: P8-15, Richland, WA 99352, USA
[b] Department of Materials Science and Engineering, University of Washington, Seattle, WA 98195, USA

**Abstract**

A continuous fiber composite was simulated by four concentric cylinders (consisting of fiber, fiber/matrix interphase coating, matrix, and surrounding composite) to explore composite stresses when irradiation swelling of the various components is included to study radial debonding at the fiber-coating interface as a function of neutron dose. SiC Type-S and Hi-Nicalon fibers, and three types of transversely isotropic carbons for the fiber coating were considered.


## 1. Introduction

SiC-based continuous-fiber composites are considered for nuclear applications as structural components due to their high specific stiffness and strength, but the differential response of the fiber, fiber/matrix interphase (fiber coating), and matrix under irradiation raises concerns [1]. A model using concentric cylindrical regions to simulate continuous fiber composites and give the composite stress distribution has been developed to explore thermo-mechanical loading effects, including irradiation swelling [2–4]. When considering a coated fiber in a surrounding matrix, four elastically distinct cylindrical regions are required [2], which can be expanded to any number of cylindrical regions [3]. Such models are used to study residual and thermals stresses in composites with a variety of fibers, matrices, and fiber coatings [2–5].

El-Azab and Ghoniem [6] modified a two-cylinder model of a continuous fiber composite to study irradiation swelling and fiber shrinkage, plus irradiation and thermal creep of both fiber and matrix, on the time-dependent stresses in a composite with SCS-6 or Nicalon fibers. They showed that Nicalon fiber shrinkage under irradiation leads to fiber/matrix debonding [7,8]. However, none of the previous studies of SiC-based continuous fiber composites under irradiation has considered irradiation-induced dimensional changes to fibers, fiber coatings, and SiC-matrices simultaneously.

## 2. Simulation details

### 2.1. Four cylinder model

A continuous fiber composite is simulated by four concentric cylinders [2]. The surrounding composite is the outermost cylinder, while the matrix, fiber coating, and fiber are the remaining cylinders, with the fiber being the innermost cylinder, denoted as domains $n = 1$, 2, 3, 4 with radii $r_1$, $r_2$, $r_3$, and $r_4$, respectively (Fig. 1). The cylinders are subjected to three independent boundary conditions; axisymmetric temperature change, $\Delta T(r)$, uniaxial applied stress, $\sigma_{0z}$, and biaxial applied stress, $\sigma_{0r}$, where $r$ and $z$ are the radial and axial components in cylindrical coordinates $(r, \theta, z)$. Stress relaxation was not allowed during irradiation or during cooling from the fabrication temperature and all components remain elastic and perfectly bonded.

* Corresponding author. Tel.: +1-509 376 1442; fax: +1-509 376 0418.
*E-mail address:* chuck.henager@pnl.gov (C.H. Henager Jr.).

0022-3115/$ - see front matter © 2004 Elsevier B.V. All rights reserved.
doi:10.1016/j.jnucmat.2004.04.110

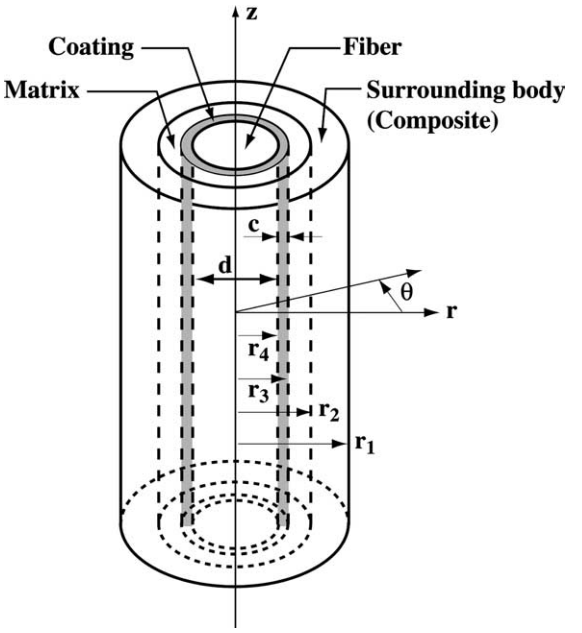


Fig. 1. Schematic of four-cylinder model showing coordinate system and identifying the four regions. Fiber has diameter $d$ and the coating has thickness $c$ and the remaining radii are computed from Eq. (4).

The elastic solution gives the axial, radial, hoop stress in all the regions ($n = 1, 2, 3, 4$) as

$$\sigma_r^n = C_{11}^n\left(A_n - \frac{B_n}{r^n}\right) + C_{12}^n\left(A_n + \frac{B_n}{r^n}\right) + C_{13}^n E_n - \beta_1^n \Delta T - \gamma_1^n, \tag{1a}$$

$$\sigma_\theta^n = C_{12}^n\left(A_n - \frac{B_n}{r^n}\right) + C_{11}^n\left(A_n + \frac{B_n}{r^n}\right) + C_{13}^n E_n - \beta_1^n \Delta T - \gamma_1^n, \tag{1b}$$

$$\sigma_z^n = 2C_{13}^n A_n + C_{33}^n E_n - \beta_3^n \Delta T - \gamma_3^n, \tag{1c}$$

where $C_{ij}^n$ are the material elastic properties, $\Delta T$ is the uniform temperature change, and $A_n$, $B_n$, and $E_n$ are the coefficients of the solutions of the four cylinder problem for the appropriate boundary conditions [2,3]. For this problem, $B_4 = 0$ and $E_n = E$ for all $n$. The terms involving $\beta_i$ are defined as

$$\begin{aligned} \beta_1^n &= (C_{11}^n + C_{12}^n)\alpha_T^n + C_{13}^n \alpha_L^n, \\ \beta_3^n &= 2C_{12}^n \alpha_T^n + C_{33}^n \alpha_L^n, \end{aligned} \tag{2}$$

where $\alpha_T$ and $\alpha_L$ are the transverse (T) and longitudinal (L) coefficients of thermal expansion for each domain. Transverse refers to in-plane properties and longitudinal refers to properties parallel to the $z$-axis. The $\gamma_i$ terms are defined in each domain as the radiation-induced stresses as

$$\begin{aligned} \gamma_1^n &= (C_{11}^n + C_{12}^n)\varepsilon_T^n + C_{13}^n \varepsilon_L^n, \\ \gamma_3^n &= 2C_{12}^n \varepsilon_T^n + C_{33}^n \varepsilon_L^n. \end{aligned} \tag{3}$$

The $\varepsilon_T$ and $\varepsilon_L$ terms are determined from swelling data for each material in the composite (see 2.2 below). For the outermost region, $n = 1$, the properties are calculated using the volume fractions of the matrix ($n = 2$), coating ($n = 3$), and fiber ($n = 4$). These are given by ratios of the various domain radii as

$$V_m = 1 - \left(\frac{r_3}{r_2}\right)^2, \quad V_c = \left(\frac{r_3}{r_2}\right)^2 - \left(\frac{r_4}{r_2}\right)^2, \quad V_f = \left(\frac{r_4}{r_2}\right)^2. \tag{4}$$

The fiber (f), matrix (m), and surrounding composite were treated as isotropic materials, while the pyrocarbon coatings (c) were considered to be transversely isotropic [3]. The four-cylinder problem is cast as eight simultaneous equations solved using standard matrix algebra [2,3]. In general, for $N$ domains there are $2N$ simultaneous equations that can be derived to solve for the unknown coefficients, $A_n$, $B_n$, ($B_4 = 0$) and $E$ [3].

### 2.2. Radiation-induced dimensional changes

Radiation swelling terms were added using parametric fits to strain (swelling) as a function of dose for the various materials and calculating stresses using appropriate elastic constants (Eq. (3)). The swelling curve of β-SiC with respect to dose for different temperatures [9,10] was fit using linear swelling ($\Delta L/L$) versus time to an exponential function as

$$\varepsilon_{SiC}[T,t] = (1/300)\left(2.86e^{36.7/T} - 5.49e^{-896/T}\right) \times \left(1 - e^{-t/(67.193T^2 - 238312T + 2\times 10^8)}\right), \tag{5}$$

where $T$ is temperature in Centigrade, $t$ is time in seconds, and the swelling is assumed to be linearly dependent on dose up to a critical dose, which saturates at constant swelling; the saturation dose being temperature dependent. This relationship was assumed for the β-SiC matrix and for Type-S SiC fibers, but this assumption has not been verified for the Type-S fibers.

For Hi-Nicalon fibers, density changes as a function of neutron dose [11,10] were converted to strain using $\frac{\Delta L}{L} = \frac{1}{3}\left(\frac{1}{\rho_1} - \frac{1}{\rho_0}\right)\rho_0$, where $\rho_0$ is the initial density and $\rho_1$ is the density after swelling (Fig. 2). The data of Kaae et al. [12,13] for the swelling of three pyrolytic carbons as function of fast-neutron fluence was converted to dpa by multiplying the fast-neutron fluence by 0.89. These

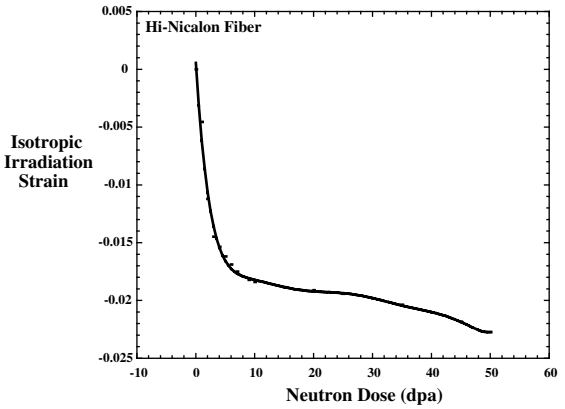


Fig. 2. Irradiation-induced strain in Hi-Nicalon fibers due to fiber densification as a function of neutron dose in dpa.

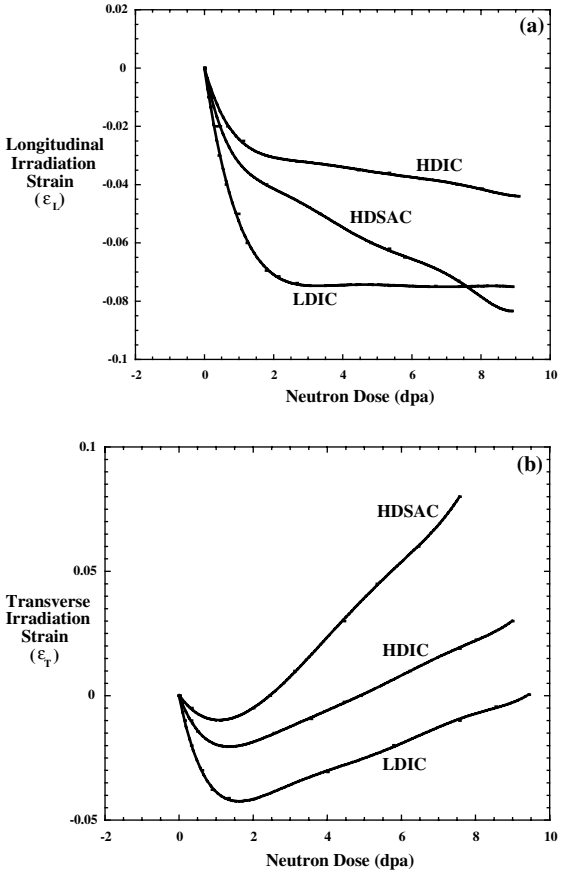


Fig. 3. Irradiation induced strain as a function of dpa for three types of pyrolytic carbon used as typical fiber coatings (HDIC, LDIC, and HDSAC). (a) Longitudinal and (b) transverse irradiation strains.

curves are shown in Fig. 3 for the three types of pyrocarbon, which are denoted as high-density isotropic carbon (HDIC), low-density isotropic carbon (LDIC), and high-density slightly anisotropic carbon (HDSAC) [12,13]. The initial density and texture determine the irradiation response of pyrocarbons, which can be tailored by controlling deposition parameters [14–16].

Six cases were studied under simulated neutron irradiation at 1000 °C using a dose rate of 0.44 dpa/year (Table 1). Two fiber types were considered: SiC Type-S and Hi-Nicalon. For each fiber type, the three types pyrocarbons were studied for fiber coatings: HDIC, LDIC, HDSAC. The assumed starting pyrocarbon densities are shown in Table 1. A residual thermal stress was present due to a $\Delta T$ of −100 °C from a nominal synthesis temperature of 1100 °C. Values of the domain radii were chosen to match microstructural information for CVI SiC/SiC composites; equivalent to a composite containing either Hi-Nicalon (HN) or Type-S fibers with a uniform fiber radius of 7 or 6 μm, respectively, and a fiber volume fraction of 0.6, which is suitable for a fiber in a bundle in typical composites [11,17–21]. The fiber coating thickness was 0.15 μm (150 nm), representative of typical pyrocarbon coating thicknesses, unless otherwise indicated. The stresses were computed starting at $t = 0$ (zero dose, only thermal stresses) out to 6 dpa.

## 3. Results and discussion

### 3.1. HN fiber composites

Large tensile radial stresses are found at the HN fiber/pyrocarbon interface regardless of the coating properties under neutron irradiation (Fig. 4), which is due to fiber shrinkage during irradiation. Although little information exists on pyrocarbon interface strengths in tension, the model predicts that stresses reach 1 GPa at 1 dpa, which should cause fiber/matrix debonding at the fiber-coating interface. Therefore, Hi-Nicalon fibers are unsuited for use as a continuous fiber in SiC/SiC composites exposed to such a radiation field, which is a well-known result [7].

### 3.2. Type-S fiber composites

Radial stresses are reduced for the Type-S fiber materials compared to the Hi-Nicalon fiber following irradiation (Fig. 5). Since the Type-S fiber responds identically (in our model) to the SiC matrix, there is no differential swelling and the response of the composite is due to the differential radiation response of the pyrocarbon coatings. Small values of the radial stress at the fiber/coating interface should retain fiber/matrix bonding up to significant neutron doses. The 150-nm HDIC pyrocarbon coating yields the smallest value of the radial stresses, with a peak stress of 120 MPa predicted after a dose of 1.5 dpa. The radial stress then decreases

Table 1
Properties used in calculations (typical values)

| Materials | Young's modulus (GPa) | | Poisson's ratio | | CTE ($10^{-6}$ $C^{-1}$) | | Temperature (°C)[a] |
|---|---|---|---|---|---|---|---|
| | Axial ($E_L$) | Transverse ($E_T$) | Axial ($\nu_L$) | In-plane ($\nu_T$) | Axial ($\alpha_L$) | Transverse ($\alpha_L$) | |
| Type-S SiC fiber | 420 | 420 | 0.2 | 0.2 | 4.0 | 4.0 | – |
| Hi-Nicalon fiber | 270 | 270 | 0.18 | 0.18 | 8.2 | 8.2 | 1000 |
| CVI SiC matrix | 460 | 460 | 0.22 | 0.22 | 4.5 | 4.5 | – |
| HDIC[b] | 80 | 80 | 0.23 | 0.23 | 5 | 5 | 1200 |
| LDIC[c] | 80 | 80 | 0.23 | 0.23 | 5 | 5 | 1200 |
| HDSAC[d] | 625 | 28 | 0.36 | 0.21 | 0 | 22 | 1200 |

[a] Temperature for which data is relevant.
[b] High-density isotropic carbon with $\rho_0 = 1.85$ g/cm$^3$.
[c] Low-density isotropic carbon with $\rho_0 = 1.65$ g/cm$^3$.
[d] High-density slightly anisotropic carbon with $\rho_0 = 1.85$ g/cm$^3$.

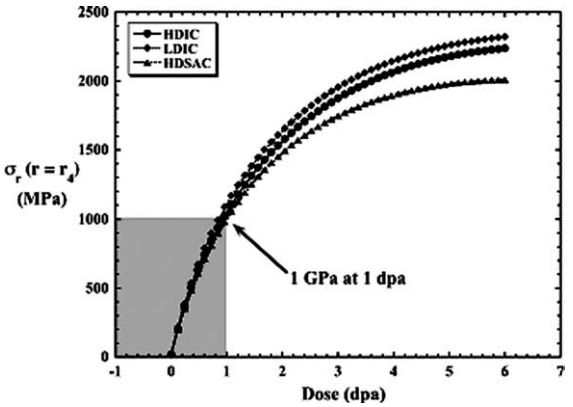


Fig. 4. Predicted radial stresses at fiber-coating interface for Hi-Nicalon fiber composites with the indicated carbon coating subjected to neutron irradiation at 1000 °C.

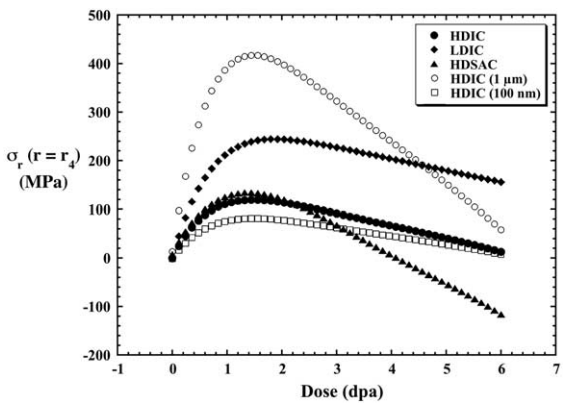


Fig. 5. Predicted radial stresses at fiber-coating interface for Type-S fiber composites with the indicated carbon coating subjected to neutron irradiation at 1000 °C.

with increasing dose corresponding to the 'turn-around' in the HDIC swelling curve. The LDIC material shrinks more than the HDIC and the peak radial stress is predicted to be about 245 MPa. The HDSAC swells more than either HDIC or LDIC and puts the system into radial compression at the fiber/coating interface. A possible concern for this coating is that continued radiation exposure may cause increasing compressive stresses that become large enough to modify composite properties. But, this deserves further study.

Changing the pyrocarbon thickness from 150 nm to 1 μm has a significant influence on the resulting radial stresses in the composite at the fiber-coating interface, since thicker coatings have larger dimensional changes compared to thinner coatings for a given strain. A 100 nm thick pyrocarbon coating further reduces the radial stress compared to 150 nm, reducing it to 80 MPa at the peak (Fig. 5). This result suggests that thinner coatings lead to improved radiation resistance. The axial stresses of these pyrocarbon coatings are quite high (in the range of several GPa) but this will have to be considered for future work. Any swelling differential between the Type-S fiber and the SiC matrix also needs to be investigated.

## 4. Conclusions

Composites containing the Hi-Nicalon fibers reach 1 GPa radial tensile stresses at the fiber-coating interface at 1 dpa independent of pyrocarbon coating type, large enough to cause interfacial debonding due to differential swelling between the HN fiber and the SiC matrix. Composites containing the Type-S fiber, for this model, have no differential swelling stresses developing between the fiber and matrix. However, differential swelling of three pyrocarbons creates small radial stresses (ranging from 80 to 245 MPa) at the fiber/coating interface, retaining fiber/matrix bonding under irradiation. Since the pyrocarbon coating properties determine the radial and axial stresses for the Type-S fiber materials,

tailoring can be explored to control composite properties by controlling the coating deposition process parameters.

## References

[1] L.L. Snead, T. Inoki, Y. Katoh, T. Taguchi, R.H. Jones, A. Kohyama, N. Igawa, in: 10th International Ceramics Congress, 2002, Part D, Adv. Sci. Technol. 33 (2003) 129.
[2] Y. Mikata, M. Taya, J. Compos. Mater. 19 (1985) 554.
[3] C.M. Warwick, T.W. Clyne, J. Mater. Sci. 26 (1991) 3817.
[4] M. Kuntz, B. Meier, G. Grathwohl, J. Am. Ceram. Soc. 76 (1993) 2607.
[5] E. Lara-Curzio, S.S. Sternstein, Compos. Sci. Technol. 46 (1993) 265.
[6] A. El-Azab, N.M. Ghoniem, Mech. Mater. 20 (1995) 291.
[7] G.W. Hollenberg, C.H. Henager Jr., G.E. Youngblood, D.J. Trimble, S.A. Simonson, G.A. Newsome, E. Lewis, J. Nucl. Mater. 219 (1995) 70.
[8] L.L. Snead, O.J. Schwarz, J. Nucl. Mater. 219 (1995) 3.
[9] R.J. Price, Nucl. Technol. 35 (1977) 320.
[10] A.R. Raffray, R. Jones, G. Aiello, M. Billone, L. Giancarli, H. Golfier, A. Hasegawa, Y. Katoh, A. Kohyama, S. Nishio, B. Riccardi, M.S. Tillack, Fusion Eng. Des. 55 (2001) 55.
[11] G.E. Youngblood, R.H. Jones, A. Kohyama, L.L. Snead, J. Nucl. Mater. 258–263 (1998) 1551.
[12] J.L. Kaae, Nucl. Technol. 35 (1977) 359.
[13] J.L. Kaae, R.E. Bullock, C.B. Scott, D.P. Harmon, Nucl. Technol. 35 (1977) 368.
[14] E. Pollmann, J. Pelissier, C.S. Yust, J.L. Kaae, Nucl. Technol. 35 (1977) 301.
[15] J.L. Kaae, Extended Abstracts and Program Biennial Conference on Carbon, 14, 1979, p. 123.
[16] J.L. Kaae, Carbon 23 (1985) 665.
[17] G.E. Youngblood, R.H. Jones, G.N. Morscher, R. Scholz, A. Kohyama, Ceram. Eng. Sci. Proc. 19 (1998) 341.
[18] R.H. Jones, C.A. Lewinsohn, G.E. Youngblood, A. Kohyama, Key Eng. Mater. 164&165 (1999) 405.
[19] H. Serizawa, C.A. Lewinsohn, G.E. Youngblood, R.H. Jones, D.E. Johnston, A. Kohyama, Ceram. Eng. Sci. Proc. 20 (1999) 443.
[20] R. Scholz, G.E. Youngblood, J. Nucl. Mater. 283–287 (2000) 372.
[21] T. Hinoki, L.L. Snead, Y. Katoh, A. Hasegawa, T. Nozawa, A. Kohyama, J. Nucl. Mater. 307–311 (2002) 1157.